Contactless and Pose Invariant Biometric Identification Using Hand Surface

Vivek Kanhangad, Ajay Kumar, *Senior Member, IEEE*, and David Zhang, *Fellow, IEEE*

***Abstract*—This paper presents a novel approach for hand matching that achieves significantly improved performance even in the presence of large hand pose variations. The proposed method utilizes a 3-D digitizer to simultaneously acquire intensity and range images of the user's hand presented to the system in an arbitrary pose. The approach involves determination of the orientation of the hand in 3-D space followed by pose normalization of the acquired 3-D and 2-D hand images. Multimodal (2-D as well as 3-D) palmprint and hand geometry features, which are simultaneously extracted from the user's pose normalized textured 3-D hand, are used for matching. Individual matching scores are then combined using a new dynamic fusion strategy. Our experimental results on the database of 114 subjects with significant pose variations yielded encouraging results. Consistent (across various hand features considered) performance improvement achieved with the pose correction demonstrates the usefulness of the proposed approach for hand based biometric systems with unconstrained and contact-free imaging. The experimental results also suggest that the dynamic fusion approach employed in this work helps to achieve performance improvement of 60% (in terms of EER) over the case when matching scores are combined using the weighted sum rule.**

***Index Terms*—Contactless palmprint, dynamic Fusion, hand biometrics, 3-D Palmprint, 3-D hand geometry, SurfaceCodes.**

I. Introduction

HAND based biometric systems, especially hand/finger geometry based verification systems are amongst the highest in terms of user acceptability for biometric traits. This is evident from their widespread commercial deployments around the world. Despite the commercial success, several issues remain to be addressed in order to make these systems more user-friendly. Major problems include, inconvenience caused by the constrained imaging set up, especially to elderly and people suffering from limited dexterity [16], and hygienic concerns among users due to the placement of the hand on the imaging platform. Moreover, shape features (hand/finger geometry or silhouette) extracted from the hand carry limited discriminatory information and, therefore, are not known to be highly distinctive.

Manuscript received October 30, 2009; revised April 18, 2010, August 02, 2010; accepted September 30, 2010. Date of publication November 09, 2010; date of current version April 15, 2011. This work was supported in part by an internal competitive research grant from The Hong Kong Polytechnic University (2009-2010), under Grant PJ70 and Grant 4-Z0F3. The associate editor coordinating the review of this manuscript and approving it for publication was Dr. Kenneth M. Lam.

The authors are with The Hong Polytechnic University, Hung Hom, Kowloon, Hong Kong (e-mail: ajaykr@ieee.org).

Color versions of one or more of the figures in this paper are available online at http://ieeexplore.ieee.org.

Digital Object Identifier 10.1109/TIP.2010.2090888

Over the years, researchers have proposed various approaches to address these problems. Several research systems have been developed to simultaneously acquire and combine hand shape and palmprint features and thereby achieving significant performance improvement. Furthermore, a lot of researchers have focused on eliminating the use of pegs used for guiding the placement of the hand. Recent advances in hand biometrics literature is towards developing systems that acquire hand images in a contact free manner. Essentially, hand identification approaches available in the literature can be classified in to three categories based upon the nature of image acquisition.

1) *Constrained and contact based*: These systems employ pegs or pins to constrain the position and posture of hand. Majority of commercial systems and early research systems [1], [2] fall under this category.
2) *Unconstrained and contact based*: Hand images are acquired in an unconstrained manner, often requiring the users to place their hand on flat surface [7], [12] or a digital scanner [5], [6].
3) *Unconstrained and contact-free*: This approach does away with the need for any pegs or platform during hand image acquisition. This mode of image acquisition is believed to be more user-friendly and have recently received increased attention from biometric researchers [3], [11], [12], [15].

Over the recent years, a few researchers have developed hand based biometric systems that acquire images in an unconstrained and contract free manner [3], [11], [13], [15]. However, none of these approaches explicitly perform 3-D pose normalization nor do they extract any pose invariant features. In other words, these approaches assume that the user's hand is being held parallel to the image plane of the camera during image acquisition, which may not always be the case, especially with such unconstrained imaging set up. Therefore, these approaches may face serious challenges when used for real world applications.

Zheng *et al.* [8] proposed a hand identification approach based upon extracting distinctive features that are invariant to projective transformations. Authors have achieved promising results on a rather small database of 23 subjects. However, the performance of their approach heavily relies on the accuracy of feature point detection on the hand images, which can deteriorate especially under large pose variations. Another drawback of their approach is that authors have not been able to utilize the palmprint information available in the acquired hand images and, therefore, the lack such highly discriminatory information may pose limitations on the scalability of their approach. The work presented in [12] is based upon the alignment of a pair of intensity images of the hand using the homographic transformation between them. Two out of four corresponding points

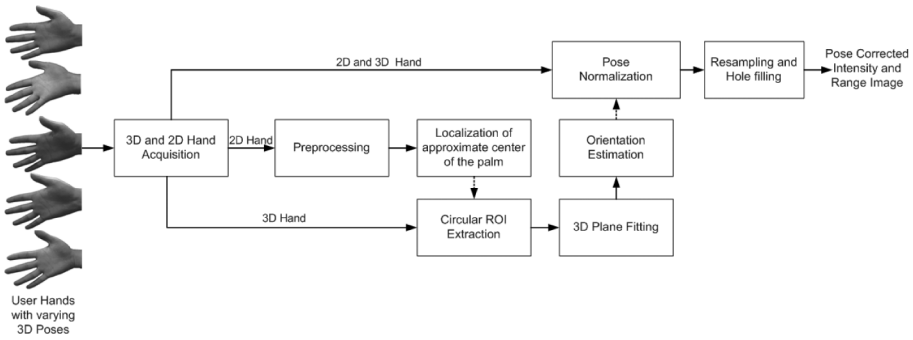

Fig. 1. Block diagram of the hand pose normalization approach.

required for the estimation of homographic transformation matrix are located on the edge map of the palmprint region. However, it should be noted that the palmprint region on the human hand lacks well defined features points and, therefore, it may not be possible to robustly estimate the homographic transformation. Moreover, even the more stable points, i.e., interfinger points used for estimating the homographic transformation cannot not always be accurately located, especially under hand large pose variations, as we show later in this paper.

As one can find in the literature, the problem of 3-D pose variation has been well addressed in the context of 3-D face [18] and 3-D ear [20] recognition. However, little work has been done in this area for 3-D hand identification, despite it being one of the highly acceptable biometric traits. The approaches proposed for 3-D face or ear recognition cannot be adopted directly as the hand identification poses its own challenges such as lack of well defined landmark points. The approaches proposed for hand pose normalization in the context of gesture recognition [23] provides only a rough estimate of the orientation of the hand. Biometric identification, on the other hand, requires accurate estimation of hand pose, since an error at the stage of alignment/registration of regions of interest would propagate and severely affect the matching performance of the system. This has motivated us to explore this area and develop an approach for pose invariant hand identification using textured 3-D hands acquired in an unconstrained and contact-free manner. The key contributions of our paper can be summarized as follows.

1) A fully automatic hand identification approach that can reliably authenticate individuals even in the presence of significant hand pose variations (in 3-D space) is presented. We utilize the acquired 3-D hand data to automatically estimate its pose based upon a single detected point on the palm. The estimated 3-D orientation information is then used to correct the pose of both the 3-D and its corresponding intensity image of the hand. The major advantage of using 3-D hand data is that the pose of the hand can be robustly estimated using only a single point (approximate palm center), unlike the existing approaches for 2-D hand identification [8], [12] that require detection of multiple landmark points on the hand.
2) Another major contribution of this paper is the proposed dynamic fusion strategy to *selectively combine palmprint and hand geometry features* extracted from the pose corrected 3-D and 2-D hand. The motivation behind such an approach emerges from our key finding (with the pose corrected hand data) that there is significant loss of hand/finger geometry information whenever the degree of rotation of the hand is considerably high. Therefore, in such cases it is judicious to ignore hand geometry information and rely only on the palmprint match scores to make a more effective decision.

Fig. 2. Localization of circular palmar region using interfmger valley points.

The rest of this paper is organized as follows. Section II provides a detailed description of our approach for 3-D hand pose estimation and correction. Section III gives a brief review of palmprint and hand geometry features extracted from the pose corrected range and intensity images. The dynamic fusion strategy for combing match scores from palmprint and hand geometry matchers is detailed in Section IV. In Section V, we introduce the 2-D-3-D hand database and present experimental results. Finally, Section VI concludes this paper with summary of our findings and the future work.

II. 3-D and 2-D Hand Pose Normalization

Fig. 1 depicts the block diagram of the proposed 3-D and 2-D hand pose normalization approach. The key idea of our approach is to robustly fit a plane to a set of 3-D data points extracted from the region around the center of the palm. The orientation of the plane (normal vector) in 3-D space is then computed and used to estimate and correct the pose of the acquired 3-D and 2-D hand.

The first preprocessing step is to localize the hand in the acquired hand images. Since the intensity and range images of the hand are acquired near simultaneously, these images are registered and have pixel to pixel correspondence. Therefore, we localize the hand by binarizing the intensity image using Otsu's threshold [4]. These binary images are further refined by morphological open operators, which remove isolated noisy regions. Finally, the largest connected component in the resulting binary image is considered to be the set of pixels corresponding to the hand. In order to locate the palm center, we initially experimented with an approach based upon interfinger (valley)

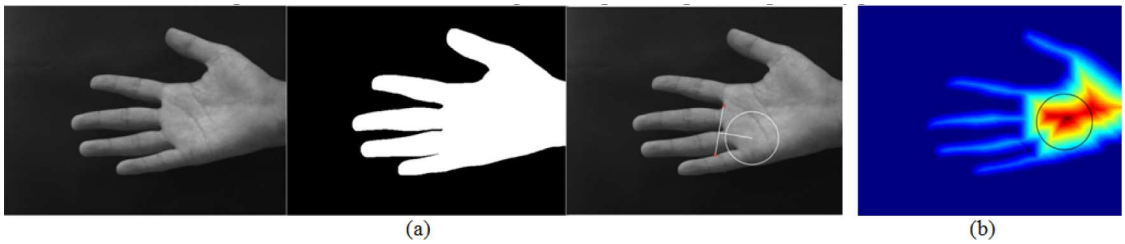

Fig. 3. (a) Incorrect localization of interfinger finger points and subsequently the center of the palm due to considerable pose variation of the hand and the resulting overlap between little and ring fingers. (b) Localization of circular palmar region using the distance transform approach.

points, commonly employed in the literature to extract the region of interest for palmprint identification. This approach traverses the foreground boundary pixels (hand contour) to detect local minima points corresponding to finger valleys between little-ring and middle-index fingers. Center of the palm is then located at a fixed distance along a line that is perpendicular to the line joining the two finger valley points. Finally, a set of 3-D data points inside a circular region around the center of the palm is extracted for further processing. Radius of this circular region of interest is empirically set to 60 pixels (in the range image). Fig. 2 pictorially illustrates the previous approach on a sample hand image in the database. This approach, however, fails to accurately detect the two interfinger points when the degree of rotation of the hand around the x axis is considerably high. This is due to the overlapping of the fingers and subsequently leads to erroneous localization of the center of the palm. Therefore, we now employ a much simpler but robust method based upon distance transform to locate the center of the palm [14]. Distance transform computes the Euclidean distance between each foreground pixel (part of the hand) and its nearest pixel on the hand contour. The point that has the maximum value for the distance transform is considered to be the center of the palm. Fig. 3 illustrates the extraction of circular ROI for a sample hand image in the database. It can be noticed that there is an overlap between fingers due to high degree of rotation. Fig. 3(a) and (b) depicts the located region of interest using the previously described approaches. Please note [refer to the third column in Fig. 3(a)] that the first approach based upon landmark points locates a point which is far off the actual center of the palm. We also observed that the approach based upon distance transform may not always locate the same palm center for different images from the same hand with varying poses. However, it still locates a point in the close vicinity of the actual center and such small error is permissible as we utilize a set of data points inside the extracted region, rather than a single feature point, for further processing.

Once a set of 3-D data points (represented by $[x_i, y_i, z_i]^{\mathrm{T}}, i = 1 \ldots m$, where m is the number of points) is extracted from the region of interest, a 3-D plane is fit using the iterative reweighted least squares (IRLS) approach. This approach solves a weighted least squares formulation at every iteration until convergence. The weighted least squares optimization at iteration p can be formulated as follows:

$$\alpha^p = \arg\min_{\alpha} \sum_{i=1}^{m} w_i^{(p-1)} \left(z_i - X_i \alpha^{(p-1)} \right)^2 \tag{1}$$

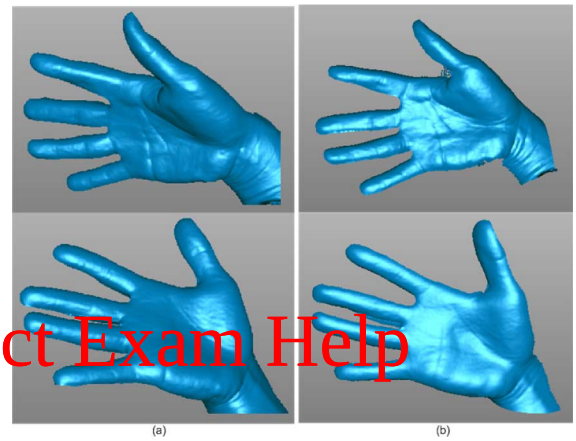

Fig. 4. (a) Shaded view of sample 3-D hand point clouds before and (b) after pose correction.

where $\alpha = [\alpha_1, \alpha_2, \alpha_3]^{\mathrm{T}}$ are the three parameters of the plane and $X_i = [1, x_i, y_i]$. The w_i is the weight given to each data point, the value of which depends upon how far the point is from the fitted plane (in the previous iteration). A bisquare weighting function is employed to assign the weights when the least squares residual (r_i) is less than a certain threshold and is defined as

$$w_i = \left(1 - (r_i)^2\right)^2 \tag{2}$$

where $r_i = (z_i - X_i \alpha)$. For points farther than the threshold, its weight is set to zero. Once the plane approximating the region around the center of the palm is computed, it is straightforward task to compute its normal vector, which gives an estimation of the orientation of the hand in 3-D space. Here we make an assumption that the human hand is a rigid plane, which may not always be true, especially in the case of inherent bend or skin deformations. Nevertheless, the IRLS approach employed here is robust and is less influenced by the outliers in the data, which in our case arise from the bend or the deformations of the hand.

Let $H_{3\mathrm{D}}$ be a $3 \times n$ matrix representing the point cloud data of the acquired 3-D hand

$$H_{3\mathrm{D}} = \begin{bmatrix} x_1 & x_2 & \ldots x_n \\ y_1 & y_2 & \ldots y_n \\ z_1 & z_2 & \ldots z_n \end{bmatrix} \tag{3}$$

where x, y and z are the three coordinates of the data points. Given this point cloud data and its orientation (in terms of the

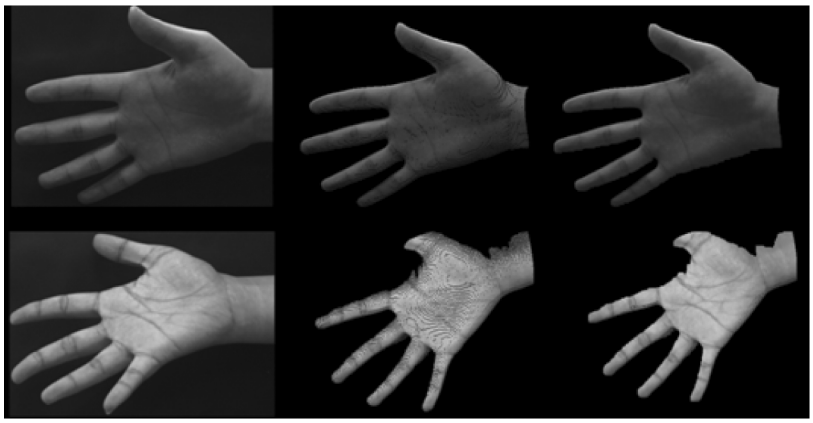

Fig. 5. (a) Sample intensity images with varying pose in our database. (b) Corresponding pose corrected and resampled images. (c) Pose corrected images after hole filling.

normal vector to the plane and represented by $\mathrm{n} = [n_x, n_y, n_z]$), the pose corrected point cloud H'_{3D} is given by

$$H'_{3D} = R\, H_{3D} \tag{4}$$

where R is the transformation matrix and can be expressed as follows:

$$R = \begin{pmatrix} \cos\theta_y & 0 & \sin\theta_y \\ \sin\theta_x \sin\theta_y & \cos\theta_x & -\sin\theta_x \cos\theta_y \\ -\cos\theta_x \sin\theta_y & \sin\theta_x & \cos\theta_x \cos\theta_y \end{pmatrix} \tag{5}$$

where $\theta_x = -\arctan(n_y/n_x)$ and $\theta_y = \arctan(n_x/n_z)$ are the rotation angles about x and y axis respectively. The rotation matrix R is also used to correct the pose of the intensity image of the hand. For this purpose, the original data can be represented as

$$H_{2D} = \begin{bmatrix} x_1 & x_2 & \ldots x_n \\ y_1 & y_2 & \ldots y_n \\ I_1 & I_2 & \ldots I_n \end{bmatrix} \tag{6}$$

where x, y are the two coordinates and $I_1, I_2, \ldots, I_n$ are the intensity values corresponding to the hand in the acquired intensity image. The pose corrected data is given by

$$H'_{2D} = R\, H_{2D}. \tag{7}$$

The pose corrected 3-D and 2-D data are a set of 3-D points (point cloud) and need to be converted to range and intensity images respectively for further processing. This is achieved by resampling the pose corrected data on a uniform grid on the x - y plane. In our experiments, the grid spacing (resolution) is set to 0.45 mm, as the x and y axes resolution of the originally scanned data is found to be around this value. The process of pose correction and resampling introduces several holes in the pose corrected range and intensity images. This is due to some regions, which are originally not visible or occluded to the scanner, getting exposed after pose correction. Therefore, besides resampling, the post processing for pose correction involves hole filling using bicubic interpolation. Fig. 4 shows the shaded view of sample 3-D hands and the corresponding pose normalized point clouds. Fig. 5 shows sample intensity hand images with varying pose in our database. The corresponding pose corrected and resampled images and the pose corrected images after hole filling are also shown in Fig. 5. As can be seen in Fig. 5(a), the hand in the third sample (refer to third row in Fig. 5) has a high degree of rotation about the x axis. The pose correction on this image leads to large number of holes in the resampled image, and loss of significant information, especially around the finger edges. It should be noted that the 3-D and 2-D hands shown in Figs. 4(b) and 5(c) have not been corrected for their pose variations about the z axis, since this process is a part of our subsequent feature extraction method.

III. Hand Feature Extraction

The pose corrected range and intensity images are processed to locate regions of interest (ROI) for hand geometry and palmprint feature extraction. The detailed description of this method, which is based upon the detection of interfinger points, can be found in [15]. It may be noted that the interfinger points can be reliably located as there can be no overlap between fingers in the pose corrected hand images. The following section provides a brief description of feature extraction approaches employed in this work.

A. 3-D Palmprint

3-D palmprints extracted from the range images of the hand (region between finger valleys and the wrist) offer highly discriminatory features for personal identification [19]. Features contained in the 3-D palmprint are primarily local surface details in the form of depth and curvature of palmlines and wrinkles. In this work, we employ the SurfaceCode 3-D palmprint representation, which is developed in our earlier work. This compact representation is based upon the computation of shape index [21] at every point on the palm surface. Based upon the value of the shape index, every data point can be classified in to one of the nine surface types. The index of the surface category is then binary encoded using four bits to obtain a SurfaceCode representation. The computation of similarity between two feature matrices (SurfaceCodes) is based upon the normalized Hamming distance.

B. 2-D Palmprint

Personal authentication based upon 2-D palmprint has been extensively researched and numerous approaches for feature extraction and matching are available in the literature. Feature extraction techniques based upon Gabor filtering has generally outperformed others. In this work, we employ the competitive coding scheme proposed in [10]. This approach uses a bank of six Gabor filters oriented in different directions to extract discriminatory information on the orientation of lines and creases on the palmprint. Six Gabor filtered images are used to compute the prominent orientation for every pixel in the palmprint image and the index of this orientation is binary encoded to form a feature representation (CompCode). The similarity between two CompCodes is computed using the normalized Hamming distance.

C. 3-D Hand Geometry

3-D features extracted from the cross-sectional finger segments have previously been shown to be highly discriminatory [15] and useful for personal identification. For each of the four fingers (excluding thumb), 20 cross-sectional finger segments are extracted at uniformly spaced distances along the finger length. Curvature and orientation (in terms of unit normal vector) computed at every data point on these finger segments constitute the feature vectors. The details of the 3-D finger feature extraction and matching are discussed in [15].

D. 2-D Hand Geometry

2-D hand geometry features are extracted from the binarized intensity images of the hand. The hand geometry features utilized in this work include—finger lengths and widths, finger perimeter, finger area and palm width. Measurements taken from each of the four fingers are concatenated to form a feature vector. The computation of matching score between two feature vectors from a pair of hands being matched is based upon the Euclidean distance.

IV. Dynamic Fusion

Weighted sum rule based fusion is widely employed in the multibiometrics to combine individual match scores. The major drawback of such a fusion framework is that poor quality samples can have adverse influence on the consolidated score since fixed weights are given for all samples. In order to overcome this problem, researchers have come up with fusion approaches that can dynamically weight a match score based upon the quality of the corresponding modality. However, accurately computing the quality of a biometric feature can be very challenging. Therefore, we develop a simple but efficient approach for combining palmprint and hand geometry scores that are simultaneously extracted from the pose corrected range and intensity images. For every probe hand, the orientation information estimated in the pose normalization step is utilized to selectively combine palmprint and hand geometry features. The motivation for such an approach arises from our observation that pose correction leads to loss of information around the finger edges and, therefore, results in incomplete (partial) region of interest for finger geometry feature extraction. The loss of crucial information in fingers is prominent when the hand is rotated about x axis. The process of matching finger/hand geometry features extracted from the pose corrected images generates poor match scores for such cases. We found from our observation that in such cases it is judicious to ignore the hand geometry information and rely only on the palmprint match scores to make a more effective decision. The proposed dynamic combination approach attempts to identify and ignore those poor hand geometry match scores using the estimated orientation of the hand. The expression for consolidated score can be given as (8), shown at the bottom of the page, where $s_{\mathrm{2DPalm}}, s_{\mathrm{3DPalm}}$ and s_{3DHG} are the matching scores from 2-D palmprint, 3-D palmprint and 3-D hand geometry matchers respectively. θ_x is the estimated angle of rotation of the hand about x axis; t^+ and t^- are the two thresholds for clockwise and counter-clockwise rotation, respectively. The weights w_1, w_2, and w_3 are empirically set to 0.4, 0.4, and 0.2 respectively. Fig. 6 shows the block diagram of the proposed pose invariant hand identification approach with dynamic fusion framework.

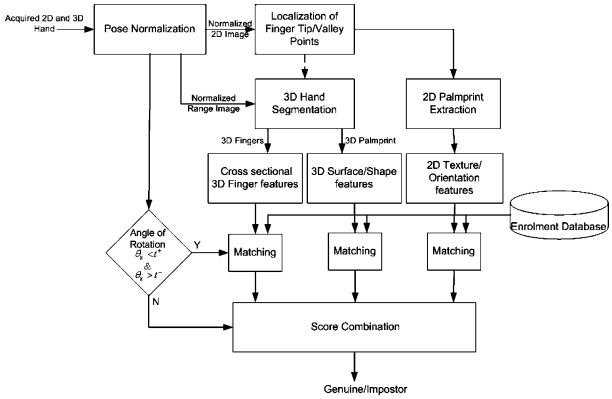

Fig. 6. Block diagram of the hand identification approach with dynamic framework for combination of palmprint and hand geometry match scores.

V. Experimental Results

A. Dataset Description

Since there is no publicly available 3-D hand database where hand images are acquired in a contact-free manner, we developed our own database using a commercially available 3-D digitizer [17]. The image acquisition system employed in this work is the same as the one described in [15]. Participants in the data collection process conducted at our institute included mainly

$$S_{\mathrm{Final}} = \begin{cases} w_1 s_{\mathrm{3DPalm}} + w_2 s_{\mathrm{2DPalm}} + w_3 s_{\mathrm{3DHG}}, & \text{if } (\theta_x < t^+) \& (\theta_x > t^-) \\ (s_{\mathrm{2DPalm}} + s_{\mathrm{3DPalm}})/2, & \text{otherwise} \end{cases} \tag{8}$$

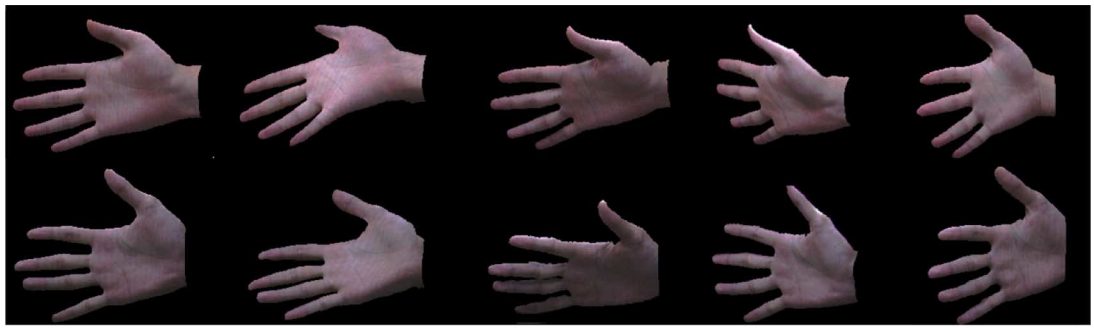

Fig. 7. Textured 3-D hands showing five different hand poses (Pose I–V) for two users (row-wise) in our database.

students who volunteered to give their biometric data. The database [22] currently contains 1140 right hand images (3-D and the corresponding 2-D) acquired from 114 subjects. In order to introduce considerable pose variations in the database, subjects were instructed to present their hand in five different poses (refer to Fig. 7). Specifically, for every user, five images are acquired in the following scenario:

1) Pose I: frontal pose where the hand is held approximately parallel to the image plane of the scanner;
2) Pose II: hand is rotated in the clockwise direction about x axis;
3) Pose III: hand is rotated in the counter-clockwise direction about x axis;
4) Pose IV: hand is rotated in the clockwise direction about y axis;
5) Pose V: hand is rotated in the counter-clockwise direction about y axis.

The amount of out-of-plane rotation (in Pose II–V) is normally not restricted and is left to the user's discretion. Users are given the freedom to pose at any angle as long as the hand is inside the imaging volume of the scanner and there is no significant overlap of fingers in the acquired images that would make it impossible to locate and separate fingers before pose correction. This is done in order to perform experiments and evaluate the performance prior to pose normalization. Table I provides the absolute mean and standard deviation of angles of rotation for each of the five poses in the database. It should be noted that the figures provided in this table are not accurate measurements (since the ground truth is not available), but are the angles of rotation estimated using the proposed approach. Nevertheless, the table gives an idea about the amount of pose variations present in our database. It can be observed that, the mean of angles about y axis (Pose IV and V) is much lower compared to the case when the hand is rotated about the x axis (Pose II and III). This is mainly due to the limitation posed by the scanner's imaging volume. During image acquisition, we observed that a user's hand cannot be scanned completely for larger angles of rotation around y axis and, therefore, we restricted the angle of rotation to ensure that the hand is held well inside the imaging volume. We also observed that the users are more comfortable while rotating their hand about the x axis. This might be the reason for higher angles of rotation about x axis (refer to Pose IV and V in Table I), when user were only instructed to rotate their hand about y axis.

TABLE I
STATISTICS OF THE 3-D HAND DATABASE

Pose	Angle of rotation about x axis (in degree)		Angle of rotation about y axis (in degree)	
	Mean	Std	Mean	Std
Pose I	6.48	4.51	5.01	3.67
Pose II	28.91	8.93	8.16	5.42
Pose III	25.99	8.88	5.42	4.798
Pose IV	13.71	8.05	15.17	10.93
Pose V	8.81	7.67	18.50	8.08

B. Verification Results

In order to ascertain the usefulness of the proposed pose correction and dynamic fusion approaches, we performed verification experiments on the acquired database. In the first set of experiments, we evaluate the performance improvement that can be achieved by employing the pose correction approach for the individual hand features. In the second set, we conduct experiments to evaluate and compare the performance of the proposed dynamic approach and weighted sum rule based fusion for hand features that are extracted from the pose corrected intensity and range images. All experiments reported in this paper follow leave-one-out strategy. In other words, in order to generate genuine match scores, a sample is matched to all the remaining samples of the user (considering them as training data) and the best match score is considered as the final score. This process is repeated for all the five samples of the user. Fig. 8(a) shows the match score distribution for 2-D palmprint features extracted directly from the acquired intensity images. It can be observed that there is a large overlap of genuine and impostor match scores due to the considerable variations in pose present in the database. Genuine and impostor score distribution for 2-D palmprint features extracted from pose corrected intensity images is shown in Fig. 8(b). It is quite clear from this figure that the process of pose normalization has greatly reduced the overlap of genuine and impostor match scores. Further, in order to ascertain this performance improvement, we computed FAR and FRR from the matching scores for the previous two cases. The corresponding ROC curves are shown in Fig. 8(c). The consistent improvement in performance (with pose correction) seen in this figure demonstrates the usefulness of the pose normalization approach for 2-D palmprint features. We also performed experiments to investigate whether similar performance improvement can be achieved for 3-D palmprint features. Match score distribution and ROC curves for 3-D palmprint matcher with

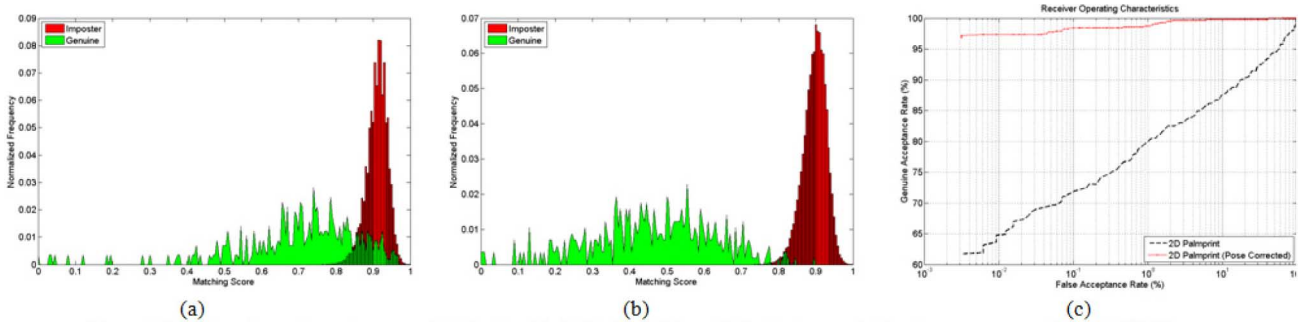

Fig. 8. (a) Genuine—Impostor score distribution for 2-D palmprint matching before and (b) after pose collection. (c) ROC curves for the 2-D palmprint matching before and after pose correction.

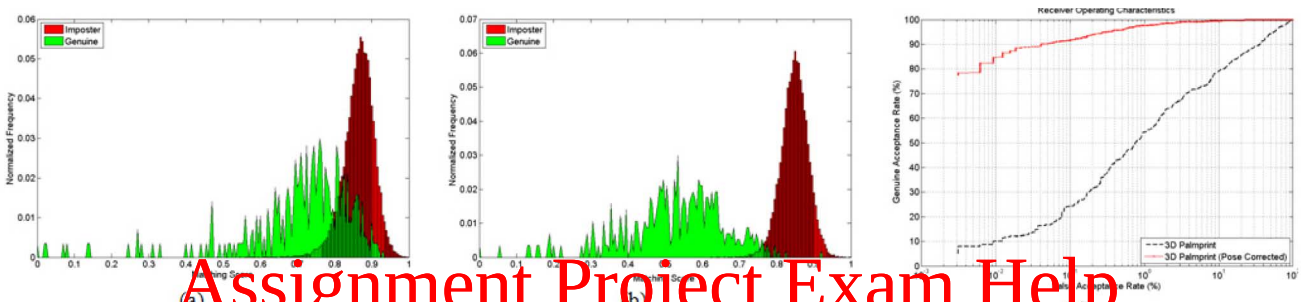

Fig. 9. (a) Genuine—Impostor score distribution for 3-D palmprint matching before and (b) after pose correction. (c) ROC curves for the 3-D palmprint matching before and after pose correction.

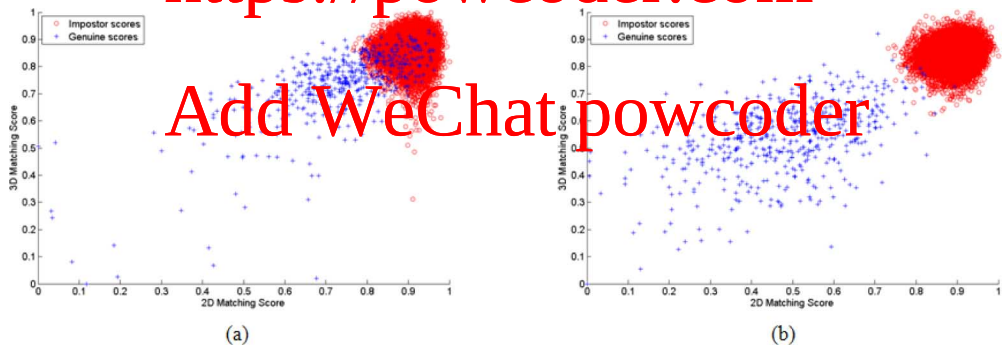

Fig. 10. (a) 2-D score distribution for 2-D and 3-D palmprint matchers before and (b) after pose correction.

and without pose correction are shown in Fig. 9. 2-D matching score distribution for 2-D and 3-D palmprint matchers shown in Fig. 10 shows significant reduction in overlap of genuine and impostor scores after pose correction. In the case of hand geometry features, 3-D features perform slightly better than 2-D features. [refer to ROC curves in Fig. 11(a) and (b)]. Table II provides a summary of this set of experiments with EER as the performance index. Finally, we evaluate the performance from the combination of palmprint and hand geometry features using weighted sum rule and the proposed dynamic fusion approach. As shown Fig. 11(c), the dynamic approach consistently outperforms the simple combination of match scores using the sum rule. Table III illustrates the equal error rates from our experiments for the combination of palmprint and hand geometry matching scores simultaneously generated from contactless 2-D and 3-D imaging.

C. Discussion

The experimental results presented in this paper are significant in the context of contact-free hand identification as it has been demonstrated that reliable identification can be performed even in the presence of severe hand pose variations. Most of the previous studies on unconstrained and contact-free hand identification do not address pose variations of the user's hand. Instead these approaches implicitly make an assumption that the user is cooperative enough to present the frontal view of his/her hand. However, in practice such approaches may require supervision in order to ensure that frontal views of the hand are acquired, especially for users who are not trained to use the system. More recently, researchers have developed hand identification approaches that yield promising performance even when the hand images are acquired under considerable

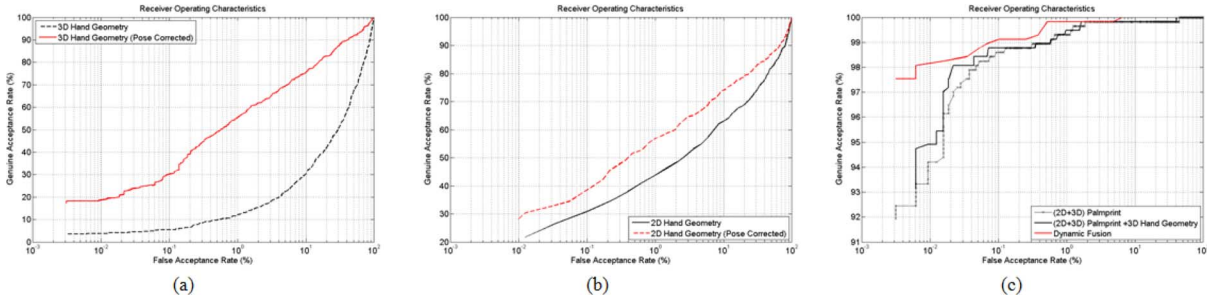

Fig. 11. ROC curves for (a) the 3-D hand/finger geometry and (b) 2-D hand geometry matching before and after pose correction. (c) ROC curves for the combination of 2-D, 3-D palmprint and 3-D hand geometry matching scores using weighted sum rule and the proposed dynamic approach.

TABLE II
EQUAL ERROR RATES OF PALMPRINT AND HAND GEOMETRY MATCHERS BEFORE AND AFTER POSE CORRECTION

Matcher	EER (%) (Without Pose Correction)	EER (%) (Pose Corrected)
2D Palmprint	11.80	1.10
3D Palmprint	16.32	1.61
3D Hand Geometry	40.9	17.2
2D Hand Geometry	28.69	22.15

TABLE III
EQUAL ERROR RATES FOR COMBINATION OF PALMPRINT AND HAND GEOMETRY FEATURES

Matcher	EER (%)
(2D+3D) Palmprint	0.72
(2D+3D) Palmprint + 3D Hand Geometry	0.71
Dynamic Fusion	0.29

pose variations. However, these approaches are based upon multiple land mark points located on the intensity images of the hand and, therefore, their performance largely relies on the accuracy of feature point detection. The approach presented in this paper exploits the acquired 3-D hand data to estimate the pose of the user's hand. The major advantage of the 3-D data is that the orientation of the hand can be robustly estimated using a single point detected on the palm. In addition, discriminatory 3-D features extracted from the pose corrected range images help to significantly improve the performance of the system when used in combination with 2-D hand features.

Experimental results from our investigation on individual hand features suggest that the palmprint features (2-D as well as 3-D) are more suitable to be utilized, especially when the degree of rotation of the hand is considerably high. This is mainly because the palmprint features are less affected by occlusion. In other words, the major part of the palmprint region is visible to the scanner (even at higher angles of rotation) and, therefore, the complete palmprint can be extracted from the pose corrected range images. On the other hand, performance of the hand geometry features has been disappointing. Although there is significant improvement in performance with the proposed pose normalization approach, the hand (finger) geometry features suffer from loss of crucial information due to occlusion around the finger edges. The occlusion is noticeably severe when the hand is rotated about the x axis as major part of finger around its edges is not visible to the scanner, resulting in significant loss of information during pose correction. Therefore, only a partial region of interest for fingers can be recovered from the pose corrected intensity and range images. Moreover, the assumption that the palm and fingers lie on a plane (coplanar) does not strictly hold good in most cases due to finger movement and bending. This also might have played a role in the poor performance of the hand geometry features.

The experimental results presented in this paper also show that 3-D hand geometry features performed slightly better than 2-D features. This is because the computation of matching distance for 3-D finger features involves a sliding approach that performs multiple matches between the cross-sectional finger features. This approach can effectively address the partial matching of fingers to certain extent. On the other hand, 2-D finger width features extracted from the pose corrected intensity images suffer the most when only partial finger is available for matching. Therefore, we do not utilize the 2-D hand geometry features in the fusion framework for the combination of hand features.

Fig. 11(c) shows the ROC curves for combination of palmprint and hand geometry features. As can be observed from this figure, a simple weighted combination of palmprint (2-D as well as 3-D) and 3-D hand/finger geometry fails to achieve the desired results. In fact, the combination achieves only marginal improvement in EER (refer to Table II) over the case when only 2-D and 3-D palmprint matching scores are combined. On the other hand, the proposed dynamic combination approach achieves a relative performance improvement of 60% in terms of EER over the case when features are combined using weighted sum rule. As discussed earlier, the dynamic fusion approach can lessen the influence of the poor hand geometry match scores on the consolidated match score and thereby it helps to improve the verification accuracy.

VI. Conclusion

This paper has presented a promising approach to achieve pose invariant biometric identification using hand images acquired through a contact-free and unconstrained imaging set up. The proposed approach utilizes the acquired 3-D hand to estimate the orientation of the hand. The estimated 3-D orientation information is then used to correct pose of the acquired 3-D as well as 2-D hand. The Pose corrected intensity and range images of the hand are further processed for extraction of multimodal (2-D and 3-D) palmprint and hand geometry features. We also introduced a dynamic approach to efficiently combine these simultaneously extracted hand features. This approach selectively combines palmprint and hand geometry features, while ignoring some of the poor hand geometry matching scores resulting from high degree of rotation of the user's hand, especially about the x axis. Our experimental results demonstrate that an explicit pose normalization step prior to matching significantly improves identification accuracy. Experimental results also demonstrate that the dynamic approach to combining palmprint and hand geometry matching scores consistently outperforms their straightforward fusion using weighted sum rule.

The major disadvantage of the proposed approach that hampers its utility for real world applications is the use of commercial 3-D scanner. Slow acquisition speed, cost and size of this scanner make it infeasible for any online biometric applications. As part of our future work, we intend to investigate alternative 3-D imaging technologies that can overcome these drawbacks. We are also exploring a dynamic feature level combination in order to further improve the performance.

References

[1] R. Sanchez-Reillo, C. Sanchez-Avila, and A. Gonzalez-Macros, "Biometric identification through hand geometry measurements," *IEEE Trans. Pattern Anal. Mach. Intell.*, vol. 22, no. 10, pp. 168–1171, Oct. 2000.

[2] A. K. Jain, A. Ross, and S. Pankanti, "A prototype hand geometry-based verification system," in *Proc. AVBPA*, Mar. 1999, pp. 166–171.

[3] S. Malassiotis, N. Aifanti, and M. G. Strintzis, "Personal authentication using 3-D finger geometry," *IEEE Trans. Inf. Forensics Security*, vol. 1, no. 1, pp. 12–21, Mar. 2006.

[4] N. Otsu, "A threshold selection method from gray-level histograms," *IEEE Trans. Syst., Man Cybernet.*, vol. 9, no. 1, pp. 62–66, Jan. 1979.

[5] W. Xiong, K. A. Toh, W. Y. Yau, and X. Jiang, "Model-guided deformable hand shape recognition without positioning aids," *Pattern Recognit.*, vol. 38, no. 10, pp. 1651–1664, Oct. 2005.

[6] S. Ribaric and I. Fratric, "A biometric identification system based on eigenpalm and eigenfinger features," *IEEE Trans. Pattern Anal. Mach. Intell.*, vol. 27, no. 11, pp. 1698–1709, Nov. 2005.

[7] D. L. Woodard and P. J. Flynn, "Finger surface as a biometric identifier," *Comput. Vis. Image Understand.*, vol. 100, no. 3, pp. 357–384, Dec. 2005.

[8] G. Zheng, C. J. Wang, and T. E. Boult, "Application of projective invariants in hand geometry biometrics," *IEEE Trans. Inf. Forensics Security*, vol. 2, no. 4, pp. 758–768, Dec. 2007.

[9] A. Kumar and D. Zhang, "Hand geometry recognition using entropy-based discretization," *IEEE Trans. Inf. Forensics Security*, vol. 2, no. 2, pp. 181–187, Jun. 2007.

[10] A. W. K. Kong and D. Zhang, "Competitive coding scheme for palmprint verification," in *Proc. IEEE Int. Conf. Pattern Recognit.*, Washington, DC, 2004, pp. 1051–4651.

[11] A. Kumar, "Incorporating cohort information for reliable palmprint authentication," in *Proc. ICVGIP*, Dec. 2008, pp. 583–590.

[12] C. Methani and A. M. Namboodiri, "Pose invariant palmprint recognition," in *Proc. ICB*, Jun. 2009, pp. 577–586.

[13] A. Morales, M. Ferrer, F. Díaz, J. Alonso, and C. Travieso, "Contact-free hand biometric system for real environments," in *Proc. 16th Eur. Signal Process. Conf.*, Laussane, Switzerland, Sep. 2008.

[14] A. Kumar and D. Zhang, "Personal recognition using hand-shape and texture," *IEEE Trans. Image Process.*, vol. 15, no. 8, pp. 2454–2461, Aug. 2006.

[15] V. Kanhangad, A. Kumar, and D. Zhang, "Combining 2-D and 3-D hand geometry features for biometric verification," in *Proc. IEEE Workshop Biometrics*, Miami, FL, Jun. 2009, pp. 39–44.

[16] A. K. Jain, A. Ross, and S. Prabhakar, "An introduction to biometric recognition," *IEEE Trans. Circuits Syst. Video Tech.*, vol. 14, Special Issue on Image- and Video-Based Biometrics, no. 1, pp. 4–20, Jan. 2004.

[17] "Minolta vivid 910 noncontact 3-D digitizer," 2008 [Online]. Available: http://www.konicaminolta.com/instruments/products/3-D/non-contact/vivid910/index.html

[18] K. I. Chang, K. W. Bowyer, and P. J. Flynn, "An evaluation of multimodal 2-D+3-D face biometrics," *IEEE Trans. Pattern Anal. Mach. Intell.*, vol. 27, no. 4, pp. 619–624, Apr. 2005.

[19] D. Zhang, V. Kanhangad, L. Nan, and A. Kumar, "Robust palmprint verification using 2-D and 3-D features," *Pattern Recognit.*, vol. 43, no. 1, pp. 358–368, Jan. 2010.

[20] P. Yan and K. W. Bowyer, "Biometric recognition using 3-D ear shape," *IEEE Trans. Pattern Anal. Mach. Intell.*, vol. 29, no. 8, pp. 1297–1308, Aug. 2007.

[21] C. Dorai and A. K. Jain, "COSMOS—A representation scheme for 3-D free-form objects," *IEEE Trans. Pattern Anal. Mach. Intell.*, vol. 19, no. 10, pp. 1115–1130, Oct. 1997.

[22] [Online]. Available: http://www.comp.polyu.edu.hk/~csajaykr/Database/3Dhand/Hand3DPose.htm

[23] L. Grieszczyk, C. Blaski, M. Chu, and J. Bouguet, "Stereo based gesture recognition invariant to 3-D pose and lighting," in *Proc. CVPR*, Jun. 2000, vol. 1, pp. 826–833.

Vivek Kanhangad received the B.E. degree in electronics and communications engineering from Visveswaraiah Technological University, Belgaum, India, and the M.Tech. degree in electrical engineering from the Indian institute of Technology, Delhi, in 2006, and is currently pursuing the Ph.D. degree at Hong Kong Polytechnic University

He is currently working as a Faculty Member at Indian Institute of Information Technology, Banglore, India. He previously worked at Motorola India. His research interests include digital signal and image processing, pattern recognition, and their applications in biometrics.

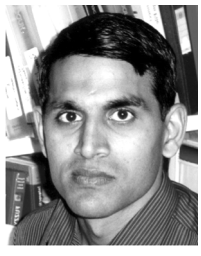

Ajay Kumar (S'00–M'01–SM'07) received the Ph.D. degree from The University of Hong Kong in 2001.

He was with the Indian Institute of Technology Kanpur and at Indian Institute of Technology Delhi, before joining the Indian Railway Service of Signal Engineers (IRSSE) in 1993. He completed his doctoral research at The University of Hong Kong in a record time of 21 months (1999–2001). He worked as a postdoctoral researcher in the Department of Computer Science, Hong Kong University of Science and Technology (2001–2002). He was awarded The Hong Kong Polytechnic University Postdoctoral Fellowship 2003–2005 and worked in the Department of Computing. He was an Assistant Professor in the Department of Electrical Engineering, Indian Institute of Technology Delhi (2005–2008). He has been the founder and lab in-charge of Biometrics Research Laboratory at Indian Institute of Technology Delhi. Since 2009, he has been working as an Assistant Professor in the Department of Computing, The Hong Kong Polytechnic University, in Hong Kong. His research interests include pattern recognition with the emphasis on biometrics and computer-vision based defect detection. He was the program chair of The Third International Conference on Ethics and Policy of Biometrics and International Data Sharing in 2010 and is the program co-chair of the International Joint Conference on Biometrics to be held in Washington, DC, in 2011.

David Zhang (SM'95–F'09) graduated in computer science from Peking University, Beijing, China, and received the M.Sc. in computer science in and the Ph.D. degree from the Harbin Institute of Technology (HIT), Harbin, China, in 1982 and 1985, respectively.

From 1986 to 1988 he was a Postdoctoral Fellow at Tsinghua University and then an Associate Professor at the Academia Sinica, Beijing. In 1994 he received his second Ph.D. in electrical and computer engineering from the University of Waterloo, Ontario, Canada. Currently, he is a Head, Department of Computing, and a Chair Professor at the Hong Kong Polytechnic University where he is the Founding Director of the Biometrics Technology Centre (UGC/CRC) supported by the Hong Kong SAR Government in 1998. He also serves as Visiting Chair Professor in Tsinghua University, and Adjunct Professor in Shanghai Jiao Tong University, Harbin Institute of Technology, and the University of Waterloo.

Dr. Zhang is the Founder and Editor-in-Chief of the *International Journal of Image and Graphics* (IJIG); Editor, Springer International Series on Biometrics (KISB); Organizer, the International Conference on Biometrics Authentication (ICBA); Associate Editor of more than ten international journals including the IEEE TRANSACTIONS AND PATTERN RECOGNITION; Technical Committee Chair of IEEE CIS and the author of more than 10 books and 200 journal papers. Professor Zhang is a Croucher Senior Research Fellow, Distinguished Speaker of the IEEE Computer Society, and a Fellow of IAPR.